

An Improved Analytic Model to Predict Fouling Phenomena in the Axial Compressor of Gas Turbine Engines

Tae Won SONG¹, Jeong Lak SOHN¹, Tong Seop KIM², Jae Hwan KIM³, and Sung Tack RO¹

¹School of Mechanical and Aerospace Engineering, Seoul National University
San 56-1, Shinlim-Dong, Kwanak-Gu, Seoul, 151-742, KOREA

Phone : +82-2-880-7434, FAX : +82-2-889-6205, E-mail : jlsohn@snu.ac.kr

²Department of Mechanical Engineering, Inha University, Incheon, KOREA

³Turbomachinery Department, Korea Aerospace Research Institute, Daejeon, KOREA

ABSTRACT

The gas turbine performance is deteriorated with increased operating hours. Fouling in the axial compressor is one of important factors for the performance degradation of gas turbine. Airborne particles entering with air into compressor adhere to the blade surface and result in the change of the blade shape, which directly influence the compressor performance. It is difficult to exactly understand the mechanism of compressor fouling because of its slowly growing process and different length scale of dimensions of compressor blades. In this study, as an approach to investigate physical phenomena of the fouling in gas turbine compressors, an improved analytic method to predict the particle motion in axial compressor and the characteristics of particle deposition onto blade is proposed. Calculated results using the proposed method and comparison with measured data demonstrate the feasibility of the model. It is also found that design parameters of axial compressor such as chord length, solidity and number of stages are closely related to the fouling phenomena. And, the particle size and patterns of particle distributions are also important factors related to the fouling phenomena in the axial compressor of gas turbine engines.

NOMENCLATURE

a_j	dimensionless deposited mass , Eq. (25)	
c	chord [m]	
C_c	slip correction coefficient, Eq. (8)	
C_x	axial velocity of fluid	[m/s]
d_p	particle diameter	[m]
E	collection efficiency	
E_c	cascade collection efficiency	
H	width of particle groups impacting on the cylinder [m]	
Kn	Knudsen number	
L	radius of cylinder	[m]
L_c	characteristic length	[m]
N	number of entering particles	
$P(d_p)$	particle distribution function	[$\mu\text{g}/\text{m}^3$]
s	pitch	[m]
Stk	Stokes number	
t	time	[second]
u	velocity vector of fluid	[m/s]
U	tangential speed	[m/s]
v	velocity vector of particle	[m/s]
v_{xi}	x -component of particle velocity at blade inlet [m/s]	
v_{yi}	y -component of particle velocity at blade inlet [m/s]	
w	relative flow velocity in blade passage [m/s]	

Greek

α	relative blade outlet angle of previous stage [degree]
β_l	flow or particle angle [degree]
β_b	stagger angle [degree]
ϕ	flow coefficient ($= C_x / U$)
μ	dynamic viscosity [kg/m-s]
ρ_p	particle density [kg/m ³]
σ	solidity ($= c / s$)
τ	relaxation time , Eq. (7)

Subscripts

b	blade
p	particle
1	in
2	out

INTRODUCTION

Performance degradation of the gas turbine is directly related to the change of the blade profile of compressor and turbine due to their deterioration caused by fouling, erosion, corrosion, and FOD (foreign object damage), etc. Among these degradation-related factors, compressor fouling, defined as the deposition process of airborne particles on compressor blades, is known as the source of about 70 ~ 85 % of performance degradation of gas turbine engines (Diakunchak, 1992). Atmosphere includes various types of airborne particles such as dirt, dust, salt, etc. that are sources of compressor fouling. Although filtration system removes most of these particles, unfiltered particles enter into compressor and, as a mixture of moisture and lubricants, adhere to the blade surface. Severe fouling problems can be resolved by installing highly efficient filters at compressor inlet, but their use is restricted due to heavy cost and large pressure drop.

In axial compressor of the gas turbine engine, fouling results in the change of the shape of leading edges of the blades and their surface roughness and, as a result, the airflow in compressor cascade becomes distorted. This brings to alter compressor characteristics. For example, as a result of compressor fouling, after 100 hour continuous operation, a low pressure compressor experienced about 3 ~ 4 % drop in a pressure ratio with 2 ~ 4 % drop in efficiency and 10 % drop in a pressure ratio with 6 ~ 7 % drop in efficiency for a high pressure compressor (Mezheritsky and Sudarev, 1998). The turbine output power decreases with the compressor performance degradation. This also results in the reduction of surge margin and dramatic unstable operation of the whole gas turbine engine.

There are many previous studies for the prediction of the overall

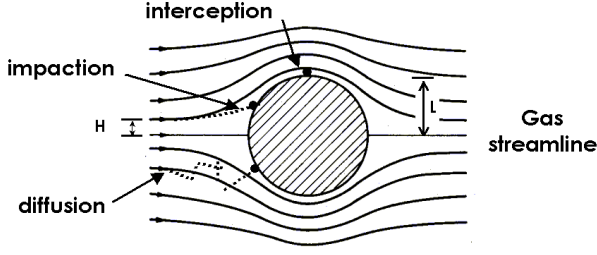


Fig. 1 Characteristics of particle motions around a cylinder

performance degradation of the gas turbine due to fouling phenomena. Saravanamuttoo and Lakshminarasimha (1985) studied the effect of fouling to the gas turbine performance by assuming only one stage (first or last stage) of the axial compressor effected by fouling. Aker and Saravanamuttoo (1989) insisted that fouling is linearly progressed along compressor stages and, as a result, the degradation of compressor stage is linearly decreased to downstream direction. Seddigh and Saravanamuttoo (1991) quantified the effect of compressor fouling to the gas turbine performance degradation. Massardo (1991) investigated the effect of fouling to pressure rise and efficiency of the axial compressor.

Tarabrin et al. (1998a) invented an analytic model of the fouling mechanism considering the motion of foulant particles by simplification of a compressor blade as a cylinder. Although this simplification is good enough, real physical phenomena such as flow conditions around a blade cannot be reflected. In the present study, a newly modified analytic model based on cylinder-based one of Tarabrin et al. (1998a) is suggested. With this model, the parametric studies of a blade profile and flow conditions are performed and the effects of a particle size and particle distribution are also investigated.

CASCADE COLLECTION EFFICIENCY

Fouling is defined as the deposition process of airborne particles on the solid surface. Figure 1 shows general mechanisms of the deposition of solid particles on a cylinder in flow field. A particle along with a streamline is diffused by a Brownian motion, or intercepted on the cylinder surface, or impacted by its inertia. When a particle floats in slow flow field, diffusion is a dominant physical phenomenon and if the particle size is no less than that of a cylinder, interception is important one (Heinsohn and Kabel, 1999). Impaction is a predominant factor in fast flow field due to inertia if a cylinder diameter is very large comparing with a particle size. In this study, it is assumed that fouling occurs only when particles impacts a cylinder (Tarabrin et al., 1998a). In order to examine the fouling effect due to impaction, the collection efficiency, E , is defined as the ratio of the number of particles impacting a cylinder to that of all particles entering perpendicular to a cylinder, as shown in Fig. 1.

$$E = \frac{\text{the number of particles impacting on a cylinder}}{\text{the number of particles entering a cylinder perpendicularly}} = \frac{H}{L} \quad (1)$$

Here, "impacting on a cylinder" means that when particles enter perpendicular to a cylinder, some particles are separated from flow field around a cylinder by their inertia and collide with a cylinder. Equation (1) assumes that the entering particles are uniformly distributed and all collided particles do not experience any bounces.

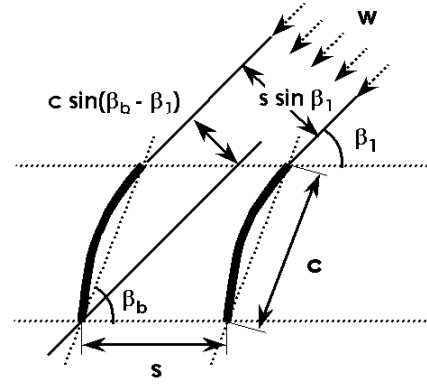


Fig. 2 Flow characteristics of between two blades in the axial compressor (Tarabrin et al., 1998a)

The collection efficiency defined in the flow field around a cylinder can be modified for the simplified cascade flow, as shown in Fig.2, around a single axial compressor blade as follows:

$$E = \frac{H}{L} = \frac{H}{c \sin(\beta_b - \beta_1)} \quad (2)$$

If considering of a blade row instead of a single blade, cascade collection efficiency based on the above expression can be defined as,

$$E_c = E \frac{c}{s} \frac{\sin(\beta_b - \beta_1)}{\sin \beta_1} \quad (3)$$

The cascade collection efficiency means that the ratio of the number of particles impacting on a blade to that of particles entering between two blades. From above two equations, it is clear that the cascade collection efficiency can be determined by blade characteristics and the width of flow field containing particles possible to impact to a blade, H . Tarabrin et al. (1998a) assumed a blade as a cylinder and H was retained using two dimensional potential flow around a cylinder and derived the cascade collection efficiency as follows:

$$E_c = (1 + 0.77 / Stk)^{-1} \frac{c}{s} \frac{\sin(\beta_b - \beta_1)}{\sin \beta_1} \quad (4)$$

where Stk denotes the Stokes number defined as

$$Stk = \frac{\tau w}{L_c} = \frac{\left\{ \rho_p d_p^2 / (18 \mu) \right\} w}{2c \sin(\beta_b - \beta_1)} \quad (5)$$

Stokes number is the ratio of particle's stopping length to its characteristic length. Zero Stokes number means that all the particles move along with flow field and there are no particles that impact to a cylinder (or a blade). When the Stokes number increases, the possibility may increase that a particle gets off flow field and impact to a cylinder (Hinds, 1982). As shown from Eq.(4), if the flow velocity at the blade inlet or its angle of attack to the blade increases, the cascade collection efficiency also increases.

A NEW ANALYTIC MODEL TO PREDICT CASCADE COLLECTION EFFICIENCY

The expression of cascade collection efficiency, Eq. (4), derived by Tarabrin et al. (1998a), has a limitation to apply to the axial compressor due to the assumption of the flow over a cylinder. In this study, a new model for cascade collection efficiency is proposed by assuming a blade as a plate instead of a cylinder. The

governing equation of a particle motion can be described as follows:

$$\tau \frac{d\mathbf{v}}{dt} + \mathbf{v} = \mathbf{u} \quad (6)$$

where, τ is the relaxation time defined as follows (Heinsohn and Kabel, 1999).

$$\tau = \frac{1}{18} \frac{d_p^2 \rho_p C_c}{\mu} \quad (7)$$

C_c in the above equation is the slip correction factor, which corrects the change of a small particle's slip in flow field (Jenning, 1988). The slip correction factor must be taken into account when micro scale particle is dealt with and can be expressed as follows:

$$C_c = 1 + Kn \left\{ 2.514 + 0.8 \exp\left(\frac{-0.55}{Kn}\right) \right\} \quad (8)$$

Since particles move in the flow field, the governing equation for the particle motion (Eq.(6)) must be solved simultaneously with governing equations of flow field, which requires numerical techniques such as computational fluid dynamics(CFD). Because of the physically complex flow field in the compressor blade row, any advanced CFD tools cannot exactly capture all important physical characteristics of the flow field. In this study, to derive a relatively simple analytic model, it is assumed that there exist infinite number of blades in an axial compressor row, and the blade shape is simplified as a plate, as shown in Fig. 3. The analysis can be categorized by two cases according to the flow characteristics between blades described as below:

Model 1: Constant Velocity Model

Assuming that the velocity between blades is not variable, the right hand side of Eq. (6) becomes constant. With x -axis set to be parallel with blades and y -axis perpendicular to x -axis as indicated in Fig.3, scalar components of Eq. (6) can be expressed as follows:

$$\tau \frac{dv_x}{dt} + v_x = w \quad (9)$$

$$\tau \frac{dv_y}{dt} + v_y = 0 \quad (10)$$

where,

$$v_x = \frac{dx}{dt}, \quad v_y = \frac{dy}{dt} \quad (11)$$

Analytic solutions of the above equations can be expressed as,

$$x = wt + \tau(v_{xi} - w)(1 - e^{-t/\tau}) \quad (12)$$

$$y = v_{yi}\tau(1 - e^{-t/\tau}) \quad (13)$$

Here, v_{xi} and v_{yi} are x and y components of particle velocity at blade inlet, respectively. Combining above two equations, an expression for the particle position between blades can be derived as:

$$x = -w\tau \ln\left(1 - \frac{y}{v_{yi}\tau}\right) + (v_{xi} - w) \frac{y}{v_{yi}} \quad (14)$$

When a particle reaches to the exit of a blade row, its position can be expressed as,

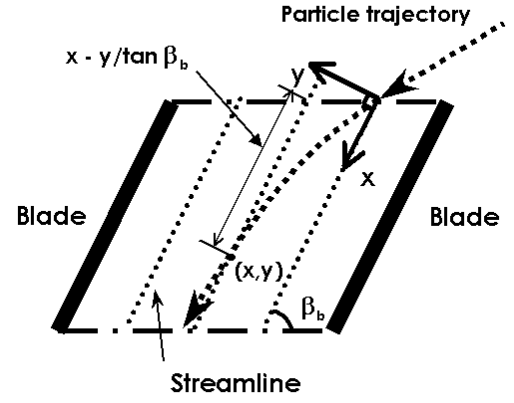


Fig. 3 Simplified cascade model with assumption of flat-plates as compressor blades

$$x = c + \frac{y}{\tan \beta_b} \quad (15)$$

From above two equations, y value of a particle at the exit of a blade row can be calculated. With this value, collection efficiency, E , and cascade collection efficiency, E_c , can be expressed as:

$$E = \frac{H}{L} = \frac{y / \sin \beta_b}{c \cdot \sin(\beta_b - \beta_1) / \sin \beta_1} \quad (16)$$

$$E_c = E \frac{c}{s} \frac{\sin(\beta_b - \beta_1)}{\sin \beta_1} = \frac{y}{s \cdot \sin \beta_b} \quad (17)$$

Model 2: Variable Velocity Model

The main function of compressor is to raise pressure by decreasing flow velocity passing through blade rows. To account for the decrease of relative flow velocity inside blade rows, this model assumes that the inlet and outlet flow velocities are satisfied with de Haller criteria ($w_2/w_1 \leq 0.72$) and flow velocity along a blade linearly decreases. With these assumptions, the x -component particle motions can be expressed as follows:

$$\tau \frac{dv_x}{dt} + v_x = w \left\{ 1 - 0.28 \frac{x - v_{yi}\tau(1 - e^{-t/\tau}) / \tan \beta_b}{c} \right\} \quad (18)$$

Solutions of the above equation can be categorized into three cases:

Case I : $D = c - 1.12\tau w > 0$

$$x = \frac{0.28\tau v_{yi} \{1 - \exp(-t/\tau)\} + c \tan \beta_b}{0.28 \tan \beta_b} + \tau \sqrt{\frac{c}{D}} \left\{ \frac{c}{0.28} (\lambda_2 \exp(\lambda_1 t) - \lambda_1 \exp(\lambda_2 t)) + \left(v_{xi} - \frac{v_{yi}}{\tan \beta_b} \right) (\exp(\lambda_1 t) - \exp(\lambda_2 t)) \right\} \quad (19)$$

where,

$$\lambda_1 = -\frac{1}{2\tau} + \frac{1}{2\tau} \sqrt{\frac{D}{c}} \quad (20)$$

$$\lambda_2 = -\frac{1}{2\tau} - \frac{1}{2\tau} \sqrt{\frac{D}{c}} \quad (21)$$

Case II : $D = c - 1.12\tau w = 0$

$$x = \frac{0.28\tau v_{yi} \{1 - \exp(-t/\tau)\} + c \tan \beta_b}{0.28 \tan \beta_b} + \exp\left(-\frac{t}{2\tau}\right) \left\{ -\frac{c}{0.28} + \left(v_{xi} - \frac{v_{yi}}{\tan \beta_b} - \frac{c}{0.56\tau} \right) t \right\} \quad (22)$$

Case III : $D = c - 1.12\tau w < 0$

$$x = -\exp\left(-\frac{t}{2\tau}\right) \left\{ \frac{c}{0.28} \cos(Dt) - \left(v_{xi} - \frac{v_{yi}}{\tan \beta_b} - \frac{c}{0.56\tau} \right) \frac{\sin(Dt)}{D} \right\} + \frac{0.28\tau v_{yi} \{1 - \exp(-t/\tau)\} + c \tan \beta_b}{0.28 \tan \beta_b} \quad (23)$$

With these solutions, collection efficiency E and cascade collection efficiency E_c can be computed by the same expressions as Equations (16) and (17).

RESULTS AND DISCUSSION

The feasibility of the proposed analytic model in this study is conducted with the 12 stage axial compressor proposed by Iwamoto et al. (1991), and results are compared with those of Tarabrin et al. (1998a and 1998b). Effects of compressor design parameters such as chord length and solidity to the fouling mechanism are examined. The role of particle sizes and their distributions on the fouling process are also investigated. The geometric characteristics and design parameters of the compressor blade considered in the present study are shown in Table 1.

Particle sizes

Figure 4 shows distributions of the cascade collection efficiency with various particle sizes. As expected, the cascade collection efficiency is increased with the increase of particle sizes. The cascade collection efficiencies predicted by a cylinder-based model of Tarabrin et al. (1998a) are larger than those by plate-based ones. This is caused by the increase of impaction of particles to cylindrical geometry, which has larger curvature than plat-plates. The reason why the collection efficiencies predicted by model 2 are larger than model 1 is due to the effect of increase of inertia force of particles caused by the decrease of flow velocity between two plates.

Blade chord and solidity

Figure 5 presents the distributions of the cascade collection ef-

Table 1. Specification of blade and velocities of compressors of Iwamoto et al. (1991)

Chord, c	7 cm
Mean radius, r_m	18.7 cm
Solidity, c/s	1.5
Flow coefficient at design point, ϕ_d	0.547
Degree of reaction	0.5
Relative outlet angle from previous blade, β_1	15°
Stagger angle, β_b	40.6°
Axial velocity	150 m/s
Blade tip speed (1st stage)	350 m/s

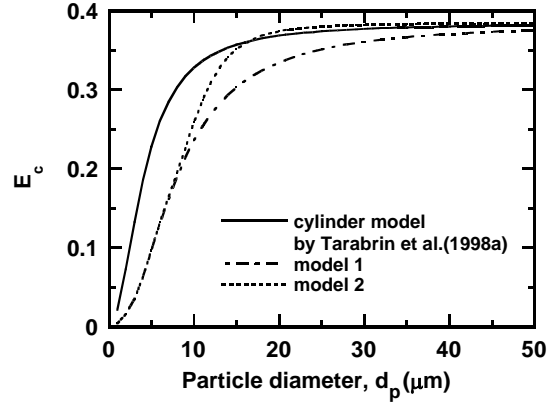


Fig. 4 Distributions of cascade collection efficiencies with various particle sizes

efficiencies with various chord lengths and particle sizes when solidity is fixed. Here, reference chord length (C_{ref}) is the chord length of compressor of Iwamoto et al. (1991). It is shown that cascade collection efficiencies are decreased with the increase of chord length. This may be caused by the decrease of probability of particle impaction on the blade due to the increase of time that particles move within flow field between blades. Figure 6 shows that the cascade collection efficiencies linearly increase with the increase of solidity when the chord length is fixed. This is not caused by the increase of particle impactions on the blades but is due to the decrease of number of inlet particles by narrowed distance between blades when the solidity is low. These results correspond with those of Tarabrin et al. (1998a). From those two figures, it is also shown that particle size is an important parameter in this study as predicted in Fig. 4.

Flow rates

As expressed in Eq. (4), the cascade collection efficiency is increased with increase of inlet flow angle (β_1) and relative flow velocity (w) at inlet. These two parameters are dependent on the magnitude of the flow rate. Figure 7 shows that the cascade collection efficiencies are decreased with the increase of flow coefficients. Here, flow coefficients are normalized by the flow coefficients at design point of the compressor of Iwamoto et al. (1991). Decrease of flow coefficient means reduced flow rate of compressor at constant rotational speed. Increase of cascade collection efficiencies with smaller flow coefficients is dominant with increased particle sizes. From these results, it can be concluded that compressor fouling will be severe when inlet air containing relatively large foulants enters into compressor with small velocity.

Compressor stages

Assuming that particles entering into a cascade are uniformly distributed and specifications of all stages of the axial compressor are the same, when particles enter into a cascade in proportion to $s \sin \beta_1$, some particles deposit on the blade surface in proportion to $E_c \sin(\beta_b - \beta_1)$. Then, the number of undeposited particles in a stage is proportional to $s \sin \beta_1 - E_c \sin(\beta_b - \beta_1)$.

As described in Figures 4~7, amount of deposited particles on the blade surface is increased when particle size is large. From this result, it is possible to think that most of large particles are deposited on the front stages and, as a consequence, number of particles entering to downstream stages is decreased. Figure 8 shows that number of particles passing through stages is decreased in downstream stages. Decrease of particle numbers in downstream stages is due to the deposition of large particles on front stages. This result tells that the fouling will be dominant especially to the front stages in axial compressor.

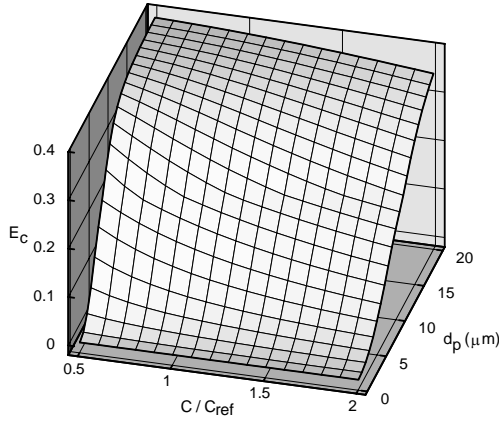


Fig. 5 Distributions of cascade collection efficiencies with various chord lengths and particle sizes ($\sigma = 1.5$)

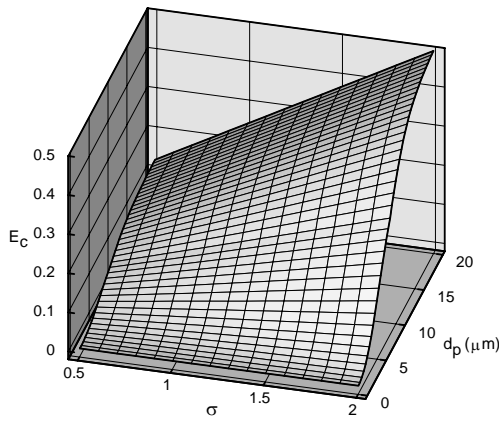


Fig. 6 Distributions of cascade collection efficiencies with various solidities and particle sizes ($c = 7\text{cm}$)

Characteristics of particle distributions

In the above discussions, it was assumed that flow entering axial compressor contains the same size of particles at each operating condition. However, in real situation, there exist various sizes of particles in atmosphere and, therefore, it is also necessary to consider distribution characteristics of particle sizes contained in inlet air. Since the distribution of particle sizes may change according to the location and time and, therefore, because of difficulty to define its accurate characteristics, effects of arbitrary particle distributions to the overall fouling mechanism are considered in this study.

In most gas turbine engines, the filtration system must be installed in front of the inlet duct to protect blades from fouling and erosion by airborne particles in the incoming air. The type of the filter determines the maximum particle diameter. Filters can be categorized such as inertial filter, self-cleaning pulse filter, high efficiency filter and etc. Among these filters, the inertial filter, which is the simplest and cheapest one, can remove particles with their diameters over $20\mu\text{m}$ (Diakunchak, 1992). In the present study, the maximum allowable particle diameter is set as 10 or $20\mu\text{m}$ depending on the filter characteristics.

For the simplicity of the analysis, it is assumed that stability time of the deposition layer, defined as the time elapsed from the beginning of particle depositions on the blade to the instant when the deposition layer is no more thickened, is the same for each stage of the axial compressor. And also it is assumed that the ratio of different particle sizes in each stage is the same as the results shown in Fig. 8. This tendency is preserved regardless of the distribution of

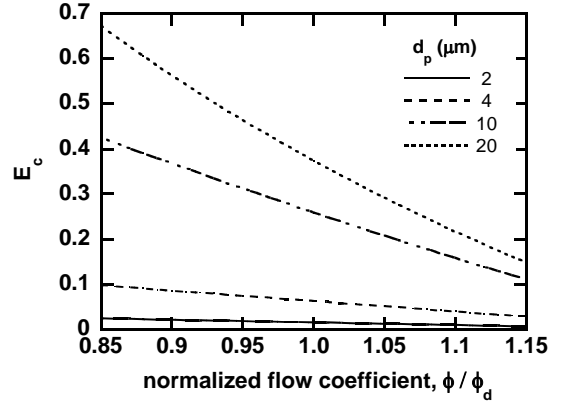


Fig. 7 Distributions of cascade collection efficiencies with various flow coefficients and particle sizes

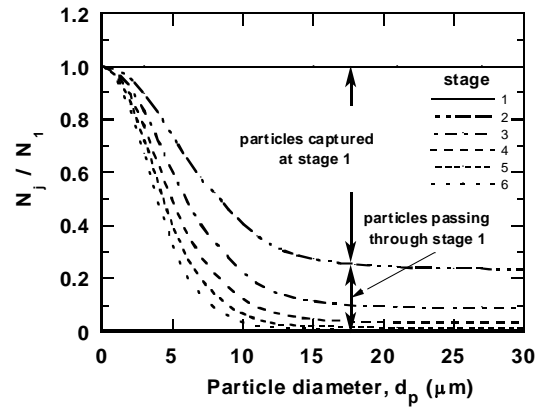


Fig. 8 Distributions of number of incoming particles in compressor stages

particle sizes of the first stage. Distributions of particle sizes of the first stage used in this study are shown in Fig. 9. Here, $P(d_p)$ means the mass [μg] of a particle with its diameter of d_p [μm] per unit volume [m^3] of air. Two kinds of maximum particle diameters such as $10\mu\text{m}$ and $20\mu\text{m}$ are chosen as described in above.

The non-dimensional collection mass of particles in each stage is defined as the collection of particle masses from the smallest size ($0.1\mu\text{m}$) up to largest one (for an example, $20\mu\text{m}$) in the stage normalized by the particle mass in the first stage. The non-dimensional collection mass of particles in the j -th stage, a_j , can be expressed as follows:

$$a_j = \frac{\sum_i (N_{i,j} - N_{i,j+1}) \cdot P(d_{p,i})}{\sum_i (N_{i,1} - N_{i,2}) \cdot P(d_{p,i})} \quad (25)$$

where, subscript i denotes i -th particle size in each stage.

Figure 10 shows non-dimensional collection masses of particles in each compressor stage with three different patterns of particle distributions with their maximum size of particle as $20\mu\text{m}$. Predictions are compared with measured data of the experimental compressor (Tarabrin et al., 1998b). Differences between measured and predicted data especially in downstream stages are due to the reduction of adhesion force of particles to the blades by the evaporation of moisture contained in air in high temperature and pressure environment. In case of dominant mass of large particles (Case A),

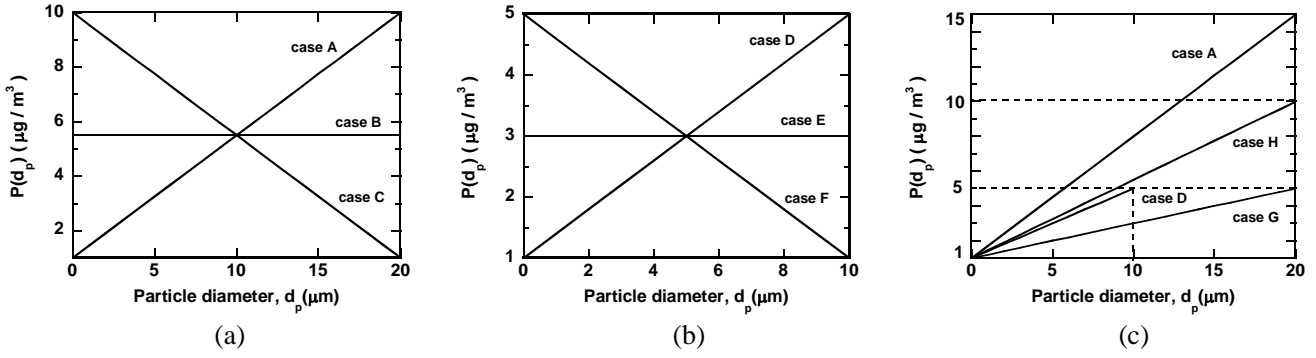


Fig. 9 Distribution patterns of particles adopted in the present study

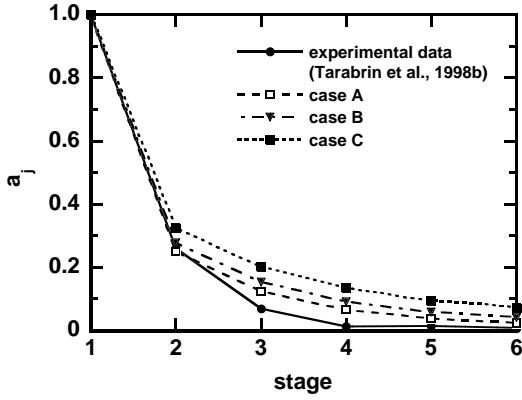


Fig. 10 Effect of distribution patterns of particles to the non-dimensional collection mass of particles with maximum particle diameter of 20 μm

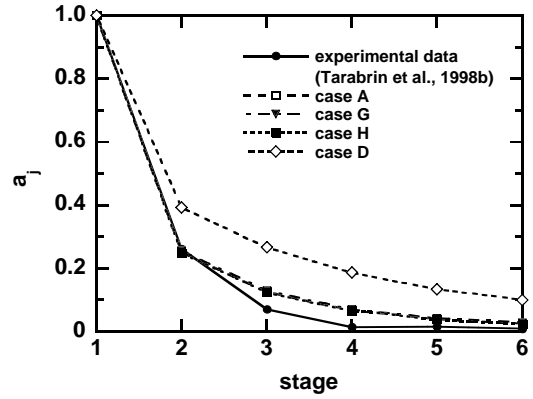


Fig. 12 Effect of distribution patterns of particles to the non-dimensional collection mass of particles with different maximum particle sizes

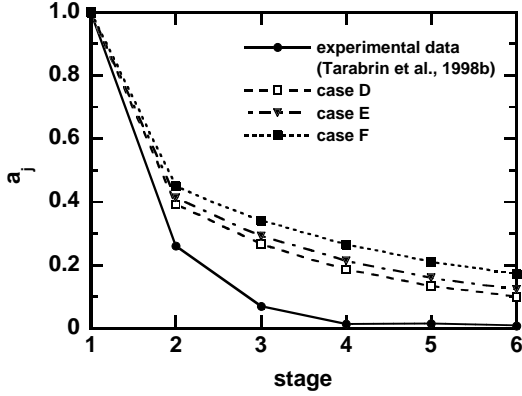


Fig. 11 Effect of distribution patterns of particles to the non-dimensional collection mass of particles with maximum particle diameter of 10 μm

most of large particles are adhered to the front stages and, as a result, non-dimensional collection masses of particles in downstream stages are relatively small. On the other hand, when the mass of small particles is dominant (Case C), in spite of the adhesion of large particles to the front stages, because of their small portion of mass, non-dimensional collection masses of particles are increased in downstream stages. Figure 11 represents similar results as Figure 10 with different size of maximum particle of 10 μm . Figure 12 shows that slope of the particle size distribution does not strongly impact to the pattern of particle adhesions on the blades. Instead, comparing with Case D, it can be concluded that the maximum size of particles, which is governed by the inlet filter, strongly influences the characteristics of particle adhesions to each stage of axial compressors.

CONCLUSIONS

An improved analytic approach based on a flat-plate model with considering variable velocity between blades has been developed for the analysis of fouling phenomena in the axial compressor of gas turbine engines. As results of parametric studies, effects of geometric parameters and flow characteristics of the axial compressor on fouling mechanism are investigated. Also, impacts of the characteristics of foulants such as their sizes and distributions on the fouling phenomena are studied. Some important conclusions disclosed by the present study are as follows:

- (1) Fouling closely related to the geometric and flow characteristics of the compressor stage. Adhesions of particles to blades, defined as the cascade collection efficiency, are increased with decrease of chord length and increase of solidity. Also, fouling is expedited with decrease of flow rates, which are closely related to the incoming air velocities.
- (2) Large particle increases the cascade collection coefficient. Deposition of large particles in front stages makes dominant fouling in front stages. Small particles pass through stages and influence downstream stages.
- (3) Distribution of particle sizes is an important parameter to determine the fouling level. Also, the maximum size of particles, which is governed by the inlet filter characteristics, plays an important role to the fouling characteristics.

ACKNOWLEDGEMENT

This work has been supported by Electric Engineering & Science Research Institute of the Ministry of commerce, industry and energy.

REFERENCES

- Aker, G. F. and Saravanamuttoo, H. I. H., 1989, "Predicting Gas Turbine Performance Degradation Due to Compressor Fouling Using Computer Simulation Techniques," *ASME Journal of Engineering for Gas Turbines and Power*, Vol. 111, pp. 343~350.
- Diakunchak, I. S., 1992, "Performance Deterioration in Industrial Gas Turbines," *ASME Journal of Engineering for Gas Turbines and Power*, Vol. 114, pp. 161~168.
- Haq, I. and Saravanamuttoo, H. I. H., 1993, "Axial Compressor Fouling Evaluation at High Speed Settings Using an Aerothermodynamic Model," ASME Paper 93-GT-407.
- Heinsohn, R. J. and Kabel, R. L., 1999, *Sources and Control of Air Pollution*, Prentice Hall, NJ.
- Hinds, W. C., 1982, *Aerosol Technology: Properties, Behavior, and Measurement of Airborne Particles*, John Wiley & Sons, Inc., NY.
- Iwamoto, T., Ikesawa, K., Kanayama, T., Nagai, K., Yukinari, A. and Nakagawa, T., 1991, "Development of a High-Pressure Ratio Axial Flow Compressor," *Proceedings of the 1991 Yokohama International Gas Turbine Congress*, Vol. II, pp.79~86.
- Jenning, S. G., 1988, "The Mean Free Path," *Journal of Aerosol Science*, Vol. 19, No. 2, pp.159~166.
- Massardo, A. F., 1991, "Simulation of Fouled Axial Multistage Compressors," *IMEchE conference on Turbomachinery*, paper C423/048, pp. 243~252.
- Mezheritsky, A. D. and Sudarev, A. V., 1998, "The Mechanism of Fouling and the Cleaning Technique in Application to Flow Parts of the Power Generation Plant Compressors," ASME Paper 90-GT-103.
- Saravanamuttoo, H. I. H. and Lakshminarasimha, A. N., 1985, "A Preliminary Assessment of Compressor Fouling," ASME Paper 85-GT-153.
- Seddigh, F. and Saravanamuttoo, H. I. H., 1991, "A Proposed Method for Assessing the Susceptibility of Axial Compressors to Fouling," *ASME Journal of Engineering for Gas Turbines and Power*, Vol. 113, pp. 595~601.
- Tarabrin, A. P., Schurovsky, V. A., Bodrov, A. I. and Stalder, J.-P., 1998a, "An Analysis of Axial Compressor Fouling and a Blade Cleaning Method," *ASME Journal of Turbomachinery*, Vol. 120, pp. 256-261.
- Tarabrin, A. P., Schurovsky, V. A., Bodrov, A. I. and Stalder, J.-P., 1998b, "Influence of Axial Compressor Fouling on Gas Turbine Unit Performance Based on Different Schemes and with Different Initial Parameters," ASME Paper 98-GT-416.